PHILOSOPHICAL TRANSACTIONS OF THE ROYAL SOCIETY A MATHEMATICAL, PHYSICAL & ENGINEERING SCIENCES

The Variability of Mixing at the Continental Slope

S. A. Thorpe, P. Hall and M. White

Phil. Trans. R. Soc. Lond. A 1990 **331**, 183-194
doi: 10.1098/rsta.1990.0064

Phil. Trans. R. Soc. Lond. A **331**, 183–194 (1990) [183]
Printed in Great Britain

The variability of mixing at the continental slope

By S. A. Thorpe, P. Hall and M. White
Department of Oceanography, The University, Southampton SO9 5NH, U.K.

The benthic boundary layer on the continental slope is a region in which isopycnal surfaces intersect topography. It is, in consequence, particularly subject to variability caused by reflecting internal gravity waves, as well as by trapped baroclinic slope waves.

Observations made using an array of moorings off the west slope of the Porcupine Bank reveal the presence there of a northerly along-slope current at depths of 3000–4000 m, which extends to some 20 km off-slope, and of waves of periods 2–9 days trapped within about 10 km (*ca.* 1 Rossby radius) of the slope. Lower-frequency variations are dominant at greater distances. The M_2 tide has a significant spectral peak, with a first subharmonic apparent near the slope. Measurements of the temperature structure in the boundary layer have been made at 1705 m on the Hebrides slope and at 3447 m off the Porcupine Bank. In both areas the boundary layer structure is dominated by asymmetrical M_2 variations in the isopycnal surfaces, with displacements of 50–100 m. Uniform near-bed 'mixed' layers appear during the tidal cycle, reaching to some 50 m off the sea bed, but are transient, lasting for only a fraction of the tidal cycle following sharp rises in isotherm levels, later to be replaced by statically stable conditions extending to within a few metres of the sea bed.

The slope-trapped waves also modify the mean temperature gradients and are responsible for variations in the locations at which reflecting internal waves of given frequency are critical or resonant.

1. Introduction

The benthic boundary layer of the deep ocean, which adjoins the continental slopes surrounding the ocean basins, is one of the most complex of the natural fluid boundary layers on the planet. Density stratification leads to an inherent non-uniformity of fluid properties in the boundary layer with increasing depth. Mean along-slope flows occur, which may be strong (20–50 cm s^{-1}) in the western boundary currents, although generally weaker (2–10 cm s^{-1}), but still present, at the eastern boundaries. The topography of the slopes, often incised by canyons and channels, is irregular, leading to a variable boundary-layer structure and even the possibility of flow separation and eddy formation in the along-slope flow (Boyer & Tao 1987). Barotropic and baroclinic, Kelvin or shelf, waves can exist, trapped within a distance of the order of the Rossby radius from the slope, and drawing largely unknown responses from the boundary layer. In practice hybrid forms of slope waves are most likely (see, for example, Huthnance 1978; Huthnance *et al.* 1986). Strong exchanges of energy from barotropic to baroclinic waves occur at the slopes, leading, in particular, to their importance as sources of internal tides with ray-like propagation offshore (Prinsenberg & Rattray 1975; Baines 1973, 1974; de Witt *et al.* 1986; Pingree & New 1989).

Internal waves incident on the slope from deep water may produce very large shear or promote static instability, for example when the gradient of the slope matches their

characteristic direction. The linear theory for two-dimensional internal gravity waves propagating in a uniformly stratified, inviscid fluid with a group velocity inclined at an angle β to the horizontal predicts that the energy density of waves reflected from a uniform slope at angle α to the horizontal increases indefinitely as β approaches α. In 'critical' conditions when $\alpha = \beta$ or, from the dispersion relation, when

$$\sin^2\alpha = (\sigma^2 - f^2)/(N^2 - f^2), \tag{1}$$

reflected waves propagate parallel to the slope (Eriksen 1985). Here σ is the wave frequency, f is the Coriolis parameter and N is the local buoyancy frequency. In laboratory experiments it is observed that, near critical conditions, vortices with horizontal axes are generated in the boundary layer when a Reynolds number of the incident waves is sufficiently small (Cacchione & Wunsch 1974), but that turbulence occurs at high Reynolds numbers (Ivey & Nokes 1989). No theory is yet available to predict the transitional conditions or the flow régime at a given Reynolds number. The amplification and enhanced shear in reflected waves at slopes when β is close to α has been proposed as a mechanism leading to enhanced boundary mixing and diapycnal diffusion, and to the modification of the internal wave spectrum (Eriksen 1985; see also Garrett & Gilbert 1988). Thorpe (1987*a*, 1988) has shown that at sufficiently small bottom slopes, less than 8.4°, reflection in non-critical conditions ($\alpha \neq \beta < 30°$) may also lead to the development of regions of static instability through nonlinear second-order resonant interactions between the incident and phase-locked reflected waves. Third-order resonances may occur if $\alpha < 11.8°$. Slope roughness may produce secondary waves that contribute to mixing (Thorpe 1989), and curvature of the mean topography may effect dissipation rates associated with breaking waves (Gilbert & Garrett 1989). Non-uniform stratification (Phillips *et al.* 1986; Ivey 1987), flows that vary in position on the slope, or varying roughness will result in there being zones of more, or less, efficient turbulence generation.

Our main aim is to describe and interpret observations that have been made at sea, so as to identify and establish a firm understanding of those processes that appear to be most important, and to extend earlier results by Thorpe (1987*b*). Few such observations have so far been reported (for examples, see Wunsch & Hendry 1972; Weatherley & Martin 1978; Eriksen 1982; Thorpe 1987*b*; and for a summary see the latter) and no comprehensive description of the slope boundary layer and its interaction with mean or variable flows is yet available.

2. Large scale variability near the continental slope

Observations were made from August 1987 to May 1988 with an array of moored vector averaging current meters (VACM; all at the same depth level) and Aanderaa current meters off the west slope of the Porcupine Bank, at positions shown by crosses in figure 1. The northerly circulation generally found close to the slope has been reviewed by Dickson & Kidd (1986) and Ellett *et al.* (1986), and some observations of variability are described by Norris & MacDougall (1986) and Thorpe (1987*b*). The along-slope current and temperature contours at the VACM level (depth 3326 m) as functions of time and distance off-slope along the line A–F′ are shown in figure 2. Allowance has been made for the mooring positions not being in a straight line by introducing a time shift to data from B and F effectively bringing the data onto the line A–F′. The time shift is calculated by estimating an appropriate phase speed from the intermediate 0.11 to 0.5 cycles per day frequency band (periods of 9–2 days respectively) of the temperature

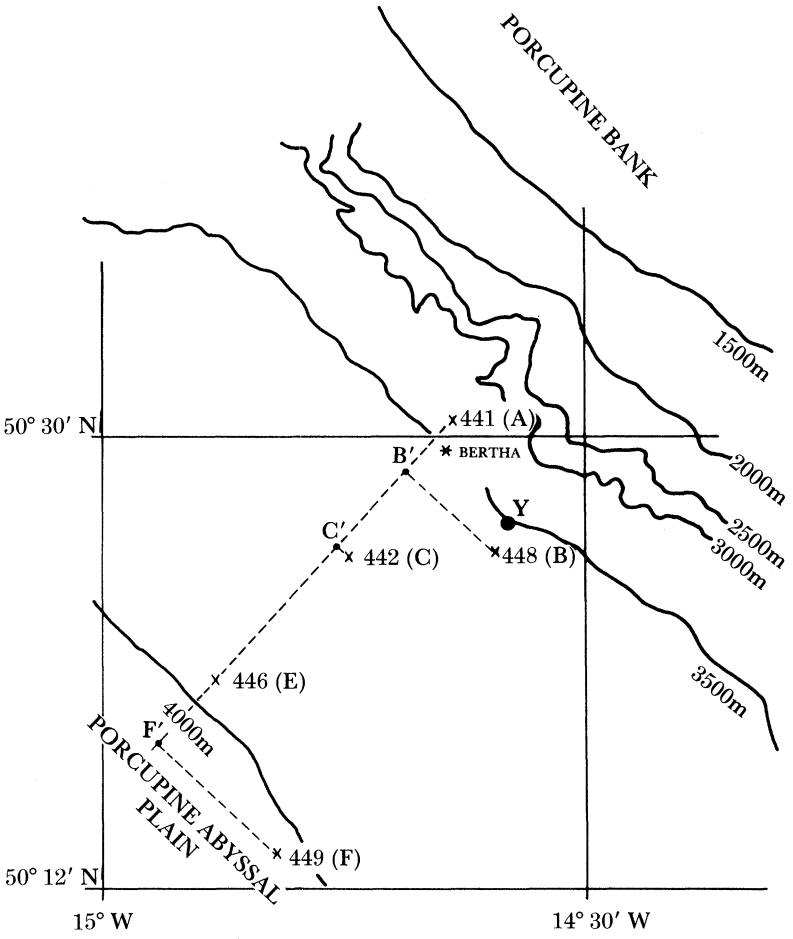

FIGURE 1. The mooring array off the west slope of the Porcupine Bank. Contour depths are shown in metres. The mooring positions have numbers and letters, A to F. The BERTHA mooring is marked with a star (see §3). Y marks the position of a 25 h long CTD yo-yo series, which will be reported elsewhere.

spectra. This results in an along-slope phase speed of 48.5 cm s^{-1} at the 4.2 day period, the phase propagating with the slope to the right. (This compares with a phase speed of 13 cm s^{-1} in the same direction estimated at the 5.45 days period by Thorpe (1987*b*).) The effective time-lags for moorings B and F are −5.07 h and −6.24 h respectively. The data were averaged over intervals of 24.84 h, or two semi-diurnal M_2 tides, and the contours were plotted from these averages.

Oscillations with periods of a few days can be seen close to the slope, and persist throughout the record both in the time series and in the contours. The motions and temperature variations associated with these oscillations appear to extend to a distance of approximately 10 km, about one Rossby radius, off slope (in figure 2*a* for example). This indicates the presence of wave motions trapped against the slope. Further from the slope at mooring F these short period fluctuations are absent, and the lower-frequency motions, with periods of tens of days and greater are more significant, an observation which is also found in the current and temperature spectra.

The along- and on-slope currents and temperatures at the VACM on mooring A are shown more clearly for comparison in figure 3. Estimates of the vertical component, ζ, of the relative

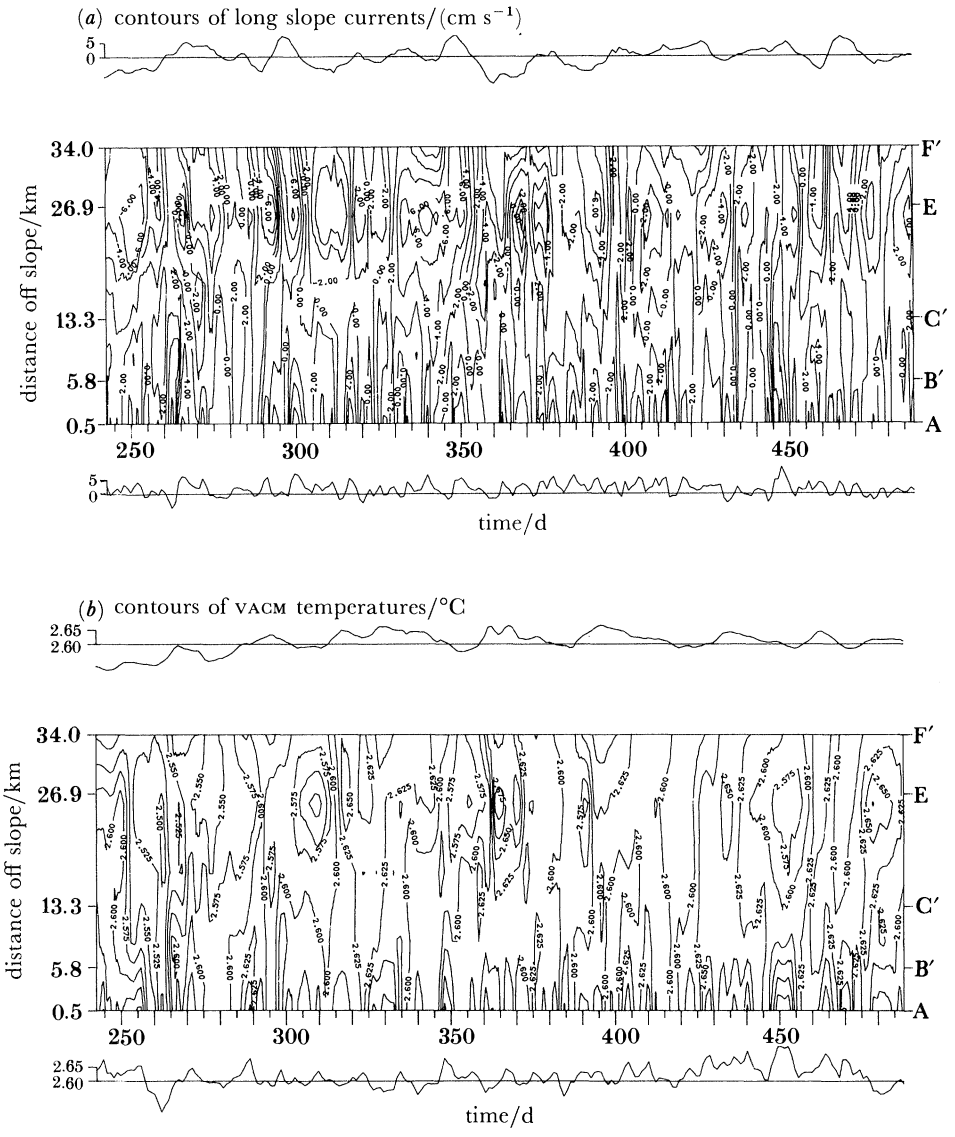

FIGURE 2. Contours of VACM measurements (3326 m depth) for (*a*) along-slope currents (direction 312°), and (*b*) temperatures, each on a time against distance off-slope frame, for data averaged over two M_2 tidal periods. Time series of the similarly averaged data at moorings A and F are shown below and above the contour plots respectively. The contour intervals are 2 cm s^{-1} and 0.025 °C.

vorticity have been made from 25 h averages of the currents measured by the VACMs on the triangle of moorings A, B and C for the period of deployment, and are also shown in figure 3. The general tendency in the area is towards positive relative vorticity due to the presence of the slope current, which should be about 3 cm s^{-1} over 20 km, or $0.015f$, where f is the local Coriolis parameter, 1.12×10^{-4} s^{-1}. The observed values, however, vary between $-0.1f$ and $+0.1f$, with a mean value of $-0.008f$. (Possible errors in the estimates are about $\pm 0.01f$.) From similar calculations Thorpe (1987*b*) obtained values in the range from $-0.09f$ to $0.17f$, and a mean value of $0.032f$. Our negative mean value may be attributed to the influence of the mean current direction at mooring B, which is being steered by the local topography (see

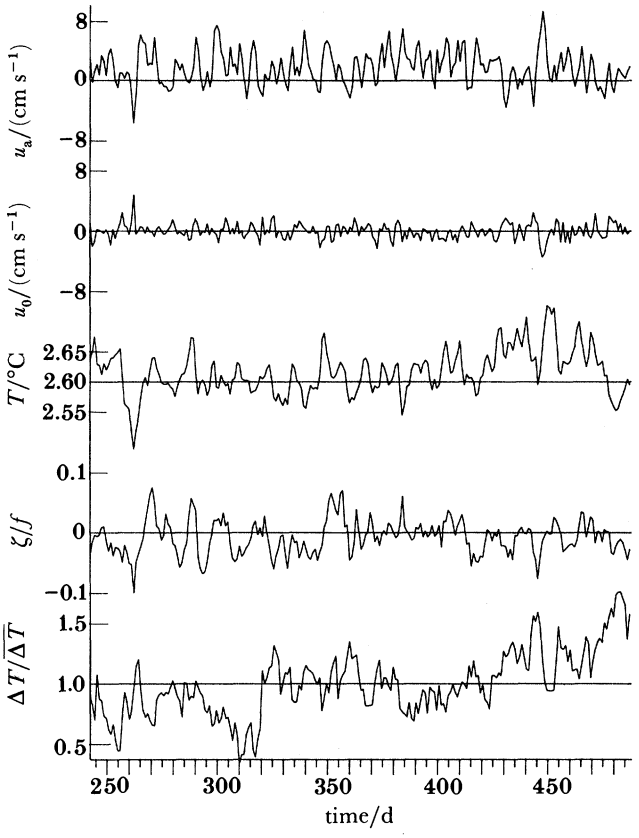

FIGURE 3. Time series (25 h averages) of (*a*) along-slope current (direction 312°) at the VACM current meter on mooring A, (*b*) on-slope current (direction 78°, perpendicular to the mean current direction) at the VACM current meter on mooring A, (*c*) temperature at the VACM current meter on mooring A, (*d*) ζ/f and (*e*) $\Delta T/\overline{\Delta T}$, ζ being the relative vorticity calculated from 25 h averages of currents at VACMs on moorings A, B and C. ΔT is the temperature difference between the VACM and the upper Aanderaa current meter both on mooring A, and $\overline{\Delta T}$ is its average value.

Owens & Hogg 1980) at a significantly different angle to the mean directions at moorings A and C (see table 1).

The corresponding time series of $\Delta T/\overline{\Delta T}$, the temperature difference (divided by its mean value) between Aanderaa and VACM current meters at the 2977 m and 3326 m depth levels respectively on mooring A averaged over 25 h intervals, is also shown in figure 3. The mean gradient increases during the observation period and fluctuates by more than 20% over periods of a few days.

The (non-averaged) vorticity spectrum shows a peak centred at approximately 6.8-day period and extending from approximately 5–8-day period. There is a corresponding peak in the temperature gradient spectrum (also non-averaged data). Comparison of the two data-sets at this 6.8-day period shows high coherence and a phase difference of −160°. A comparison between the along-slope current at the VACM on mooring A and the temperature gradient gives a very similar result with a phase difference of +170° at the 6.8-day period.

TABLE 1. CURRENT-METER DATA FOR THE PORCUPINE BANK ARRAY

(See figure 1; A, Aanderaa: V, vector averaging current meter.)

mooring	depth of water/m	instrument no.	type	start/ finish	height (off-bottom)/m	mean velocity (cm s^{-1})	mean direction	mean temperature °C	mean kinetic energy (cm s^{-1})^2
50° 30.78′ N 14° 38.26′ W	3347	44101	A	12 Aug 87 4 May 88	370	3.81	329°	2.821	23.02
		44102	V	10 Aug 87 6 May 88	21	2.12	348°	2.615	22.41
50° 25.48′ N 14° 35.60′ W	3552	44802	V	25 Aug 87 6 May 88	227	1.32	297°	2.615	13.96
50° 25.25′ N 14° 44.72′ W	3697	44201	A	12 Aug 87 4 May 88	727	1.78	346°	2.791	19.69
		44202	V	10 Aug 87 6 May 88	374	0.99	347°	2.597	16.22
		44203	A	12 Aug 87 4 May 88	22	2.67	348°	2.548	34.15
50° 20.15′ N 14° 53.10′ W	3964	44601	A	20 Aug 87 4 May 88	992	0.46	16°	2.782	21.17
		44602	V	25 Aug 87 6 May 88	636	0.54	148°	2.596	22.23
		44603	A	20 Aug 87 4 May 88	287	0.61	156°	2.531	34.03
50° 13.35′ N 14° 50.23′ W	4026	44901	A	20 Aug 87 4 May 88	1054	0.82	24°	2.753	15.49
		44902	V	25 Aug 87 6 May 88	700	0.60	75°	2.603	18.86
		44903	A	20 Aug 87 4 May 88	347	0.18	106°	2.572	22.80

3. BOUNDARY LAYER MEASUREMENTS

3.1. *The moorings*

Measurements of temperature and currents have been made close to the sea bed in two regions of continental slope, west of the British Isles. One site is on the slope of the Hebrides shelf near 58° 20′ N, 9° 45′ W in a water depth of 1705 m, and the other is on the west slope of the Porcupine Bank at a water depth of 3447 m and in the area described in §2 (see figure 1). Currents were measured, close to and remote from the slope bottom, with conventional VACMS and Aanderaa current meters. Temperatures were measured using BERTHA, a benthic resistance thermometer array (see Thorpe 1987*b*).

3.2. *Hebrides slope*

The local bottom slope here is about 4°, and was measured from an echo sounder transect made across the slope, and is close to the critical slope for the M_2 baroclinic tide. The internal Rossby radius is 5 km for this region. The mooring was deployed for a period of 550 h, from 11 May 1987 and useful data were recovered for 75 h from all 11 sensors in the BERTHA array, and 550 h from the current meters.

The mean current is northerly, following the local isobaths in the bottom 200 m (see table 2), and is consistent with earlier observations (Huthnance 1986). The increased magnitude of the northerly current in the bottom 200 m suggests the presence of a boundary current, but

there is, however, a decrease in mean current at 5 m possibly attributable to the presence of a frictional layer close to the sea-bed. The current fluctuations are dominated by the semi-diurnal barotropic tide. Currents are generally stronger than those found off the Porcupine Bank (§2) but also show reversals of period about 4–5 days. There is an apparent correlation between the direction of the along-slope flow and the near-bottom temperature gradient, which is most readily apparent in the boundary region (lower 100 m). There is a higher temperature gradient in the bottom 100 m when the flow is southerly. The total change in temperature gradient is between 0.5–2.2 times the average temperature gradient, whereas the along-slope current varies from 20 cm s^{-1} to -16 cm s^{-1}.

Gradient Richardson numbers have been calculated using the data at the 5 m and 101 m

TABLE 2. CURRENT-METER DATA FOR THE HEBRIDES SLOPE ARRAY

(Abbreviations as table 1.)

mooring	water depth/m	instrument no.	type	start/ finish	height (off-bottom)/m	mean velocity (cm s^{-1})	mean direction	mean temperature °C	mean kinetic energy (cm s^{-1})^2
58° 19.2′ N 09° 44.9′ W	1705	42801	A	11 May 87 3 June 87	1000	11.43	184°	8.647	79.31
		42802	A	11 May 87 3 June 87	500	8.17	208°	6.172	45.66
		42803	A	11 May 87 3 June 87	200	11.71	351°	4.513	95.13
		42805	V	11 May 87 3 June 87	101	12.20	009°	2.201	118.36
		42806	V	11 May 87 3 June 87	5	10.74	355°	2.020	85.92

levels, assuming that the T–S relation holds constant so that potential density can be calculated, and averaged over 43 M_2 tidal cycles. The minimum Richardson number is found at the peak in the along-slope current and is coincident with the peak in the shear. At this time the main contribution in the shear is from the along-slope current component. There is a large phase difference in the on-slope current at 5 and 101 m indicating a baroclinic component to the currents. This phase difference provides the largest component to the shear when there is an on-slope flow at 101 m, but the total shear then is much smaller than at times of peak along-slope currents.

Figure 4 shows contours of (5 min averaged) potential temperature for a 25 h period of the BERTHA deployment. Sensors were located at heights of 1.5, 4, 8, 13, 20, 30, 40, 50, 70, 90 and 110 m above the sea bed. An asymmetrical wave-like structure of M_2 period, very similar to that reported earlier (Thorpe 1987*b*) on the Porcupine slope, is observed with an amplitude (half height) exceeding 50 m. A rapid rise in the contours (temperatures falling at fixed sensors) is followed by a more gradual decrease in the contours (increasing temperatures). Water colder than any present at the commencement of the period appears as the isotherms rise sharply, indicating on-slope advection of deeper water. The period of rising isotherms is associated with a much reduced near-bottom temperature gradient. Layers of constant potential temperature, or regions where potential temperature measured between neighbouring BERTHA sensors increases with increasing depth (see figure 4*b*), are observed to reach heights of between 30–50 m above the sea bed. These mixed layers develop about 1–3 h after the times at which

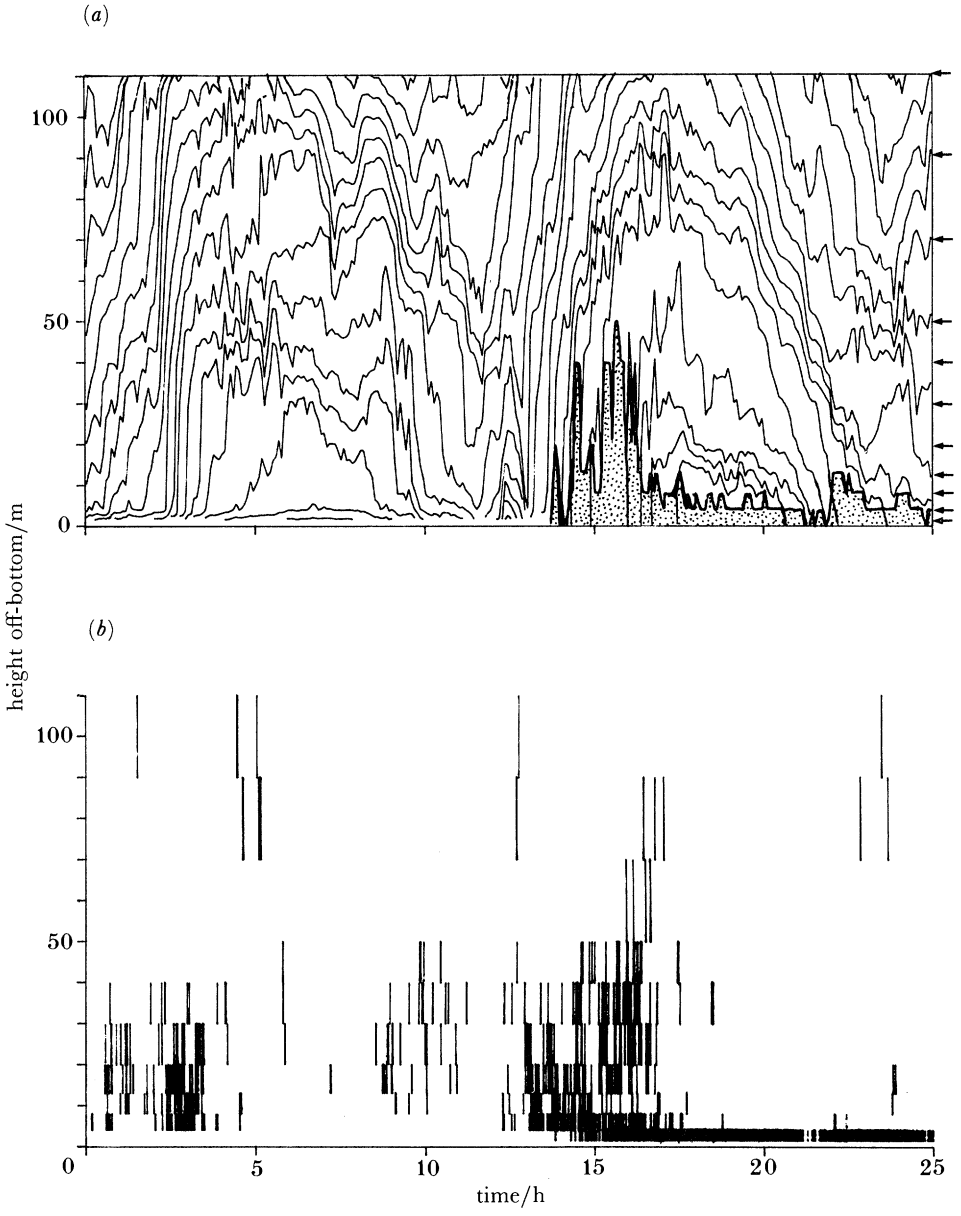

FIGURE 4. (*a*) 25 h time series of potential temperature contours, as measured by BERTHA, averaged over 5 min. The contour interval is 20 mK, and the arrows indicate the sensor locations. The stippled region shows the extent of the bottom uniform (or inverted) potential temperature layer. The height of the uniform layer is defined as the maximum height to which the potential temperature is within 1 mK of that of the lowest sensor. (*b*) Positions of potential temperature inversions between neighbouring BERTHA sensors. An inversion is recognized only if the temperature at the lower sensor is more than 3 mK greater than that of the upper sensor.

the minimum Richardson numbers are observed, a delay of the order of the mean buoyancy period (1.75 h). The layers develop and collapse rapidly (figure 4) although there is evidence that the mixing proceeds upwards from the sea bed. A mixed layer does not persist at any level throughout the period of the deployment. The temperatures at the lowest two sensors at 1.5 m and 4 m, however, are indistinguishable for about a third of that time suggesting that a mixed layer may, close to the sea bed, be a common but intermittent feature. The overall pattern is one of the periodic appearance of near-bottom regions where the potential temperature is

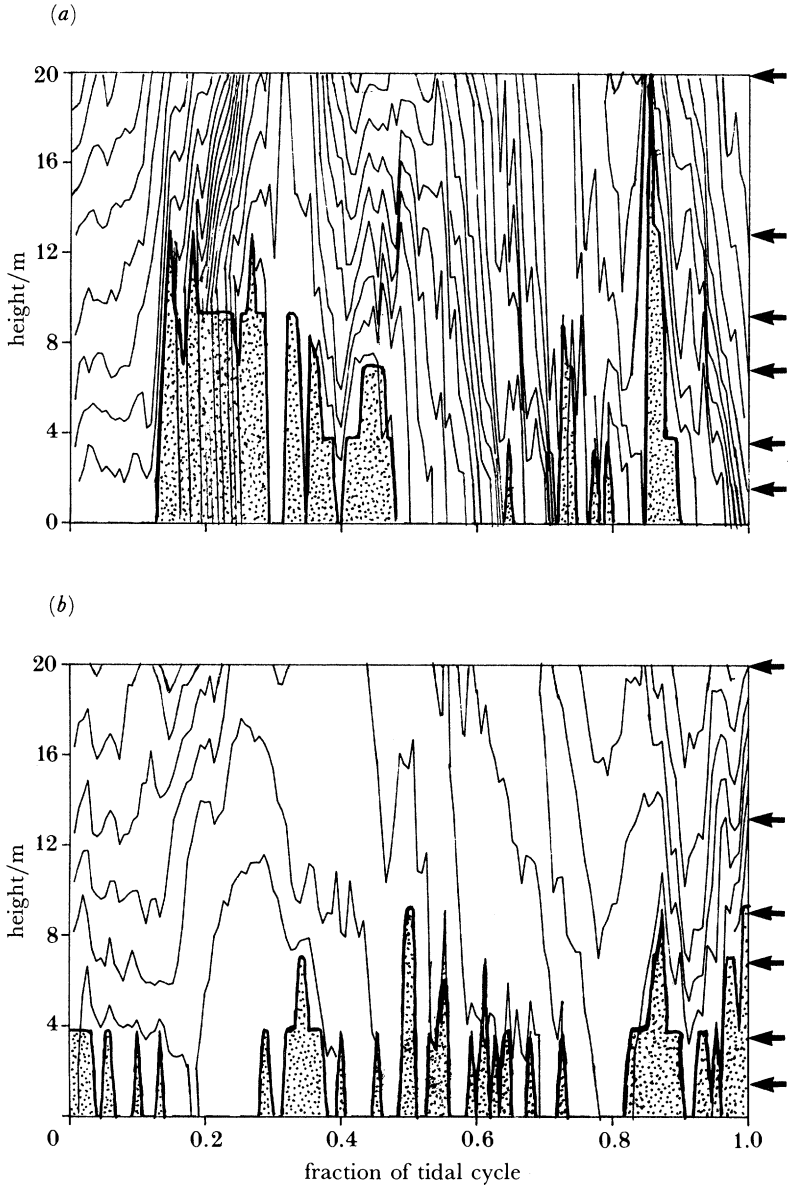

FIGURE 5. Potential temperature contours, for the Porcupine Bank, for two individual M_2 tidal cycles that have different characteristics; (*a*) high temperature gradient and (*b*) low temperature gradient. Averages taken over 5 min and contoured at (*a*) 5 mK intervals and (*b*) 3 mK intervals. The stippled region is as in figure 4, and the arrows indicate the sensor locations.

uniform (or increases with depth; static instability) as the mean temperature falls and the crest of the wave is reached. Stable stratification is re-established quickly and, except close to the boundary, is generally sustained, as temperatures rise.

3.3. *Porcupine Bank*

The position of the BERTHA mooring is shown in figure 1, and was deployed for 225 h from the 16th August 1987, with 165 h of useful BERTHA data recovered. The BERTHA sensors were located at heights of 1.5, 3.8, 7, 9.3, 13 and 20 m above the sea bed, to establish more clearly the near sea-bed structure of the boundary layer. The mooring also included 5 VACMS spanning

the bottom 170 m. The bottom slope here is about 2° and N is on average about 8×10^{-4} s^{-1}. Internal waves of about 15 h are, from (1), critical, and this is well away from the semi-diurnal period. The values for the slope angle and mean buoyancy frequency imply a condition close to second-order resonance for internal (M_2) tide reflection (Thorpe 1987*a*, and see §1).

Figure 5 shows potential temperature contours for two M_2 periods, which characterize periods of small and large temperature gradient. Features similar to those on the Hebrides slope, are found. The asymmetrical character of the wave and the low temperature gradient at the wave crest is observed, and on-slope advection is again indicated by the appearance of colder water as contours rise. One noticeable difference from the Hebrides region is the height to which uniform potential temperature layers reach when mixing occurs. Here uniform layers extend to a smaller height from the sea bed, reaching 20 m on only one brief occasion and no higher than 13 m in the two examples of figure 5. For the low temperature gradient example (figure 5*b*) the near-bottom uniform layer has a more even temporal distribution than in the high temperature gradient tidal cycle.

For both periods the near-bed structure does not vary smoothly in time and small-scale oscillations and abrupt changes in temperature are observed throughout the tidal cycle. High frequency, coherent fluctuations are observed spanning, at times, the whole BERTHA array, e.g. at phase 0.4–0.5 in figure 5*a* and phase 0–0.1 in figure 5*b*. These have a period of order 20–40 min and an inferred horizontal wavelength of 30–100 m. Patches of colder water appear at the sea bed (e.g. at phases 0.8 and 0.9 in figure 5*a*) usually when the contours are falling. These persist for about one hour, corresponding to horizontal scales of about 200 m, and extend to 5–20 m above the sea bed.

4. Discussion

Measurements made at two sites on the continental slope and rise to within 1.5 m of the sea bed have demonstrated that the benthic boundary layer, as defined by the temperature structure, is highly variable over short periods of time, in sharp contrast to that overlying abyssal plains, where near-bed 'mixed' layers persist for sometimes ten days or more until modified by fronts associated with meso-scale eddies in the overlying water (Armi & D'Asaro 1980; Thorpe 1983). Whereas near-uniform layers with evidence of frequent static instability over vertical scales of 10 m, symptomatic of large turbulent eddies, sometimes extend to about 50 m from the sea bed, within a few hours or so, at best, only a shallow (less than 5 m thick) mixed layer can be detected. The principal variations in structure are found at frequencies close to that of the M_2 tide, a probable consequence of both a large barotropic component at this frequency and of bottom slopes which are fairly close to those at which M_2 baroclinic waves are critical or resonant. The width of the response bands for both critical and resonant waves (§1) is about 1° in slope angle α, so that perfect matching of the slope and wave propagation angles is not necessary to produce significant amplification in the reflected components.

The boundary layer is most developed at about one buoyancy period after the current reaches its maximum and the Richardson number is minimum. The overall variations in thermal structure during the tidal period (figures 4 and 5), for example the rapid rise in isotherms before the establishment of a uniform near-bed layer and the enhanced near-bed gradients which form later, are in accordance with the temperature cycle produced during

reflection of internal waves from a boundary in laboratory experiments and in theoretical studies (see Thorpe 1987*a*, figs 12 and 3 respectively). The presence of tidal harmonics in the velocity and temperature spectra cannot however be accounted for within the simple, finite-amplitude, internal wave model having speed and density components that are sinusoidal in time, unless the interactions of incident and reflected waves (i.e. nonlinear terms), or perhaps non-uniform slope and buoyancy period, are included. Although present evidence suggests that on-slope propagation of a baroclinic M_2 component is responsible (Thorpe 1987*b*), at least in the Porcupine Bank area, the sources of tidal energy have not been identified and a more complete study is merited. No theoretical model is yet available that can predict, or assess the consequences of, the regions of static instability that are observed. Their presence shows that dynamic and irreversible processes are at work, beyond those associated with wave reflection and isopycnal steepening.

The temperature gradient near the sea bed is observed to vary substantially over periods of 5–8 days. The correlations found in §2 between temperature gradient, along-slope current and vorticity in this frequency band are consistent with the conservation implied by Ertel's theorem (Gill 1982). A linearized form can be written (Müller 1988)

$$(1+\zeta/f)\,\Delta T/\overline{\Delta T} = \text{const.}, \tag{2}$$

provided that the T–S relation is maintained as expected over these relatively short timescales. Variation in ζ/f should thus be 180° out of phase with $\Delta T/\overline{\Delta T}$, as observed. The amplitude of the fluctuations in ζ/f and $\Delta T/\overline{\Delta T}$ are however somewhat different. Although comparable in figure 3, at least in the frequency band of interest here, data from the Hebrides slope point to possibly much greater fluctuations in $\Delta T/\overline{\Delta T}$ near the sea bed. If confirmed in the Porcupine Bank area, these may derive from the vorticity being estimated on a scale that is not sufficiently small, or perhaps that, in the boundary layer region where dissipation may be large, the assumptions of Ertel's theorem are not valid.

The changes of N^2 of 20 % observed at the Porcupine Bank over a vertical distance of 349 m (figure 3) are found (from (1)) to imply changes in critical slope of 10 %. At the mooring site $\alpha \approx 2°$ and $\mathrm{d}\alpha/\mathrm{d}z \approx 5\times10^{-3}$ deg m^{-1} (Thorpe 1987*b*, fig. 2), where z is the depth, and hence the critical depth changes by some 40 m, or horizontally by 1.1 km. The presence of the slope waves may thus vary the tuning of local conditions favourable to wave amplification and tend to broaden the location of the most intense bottom mixing and high current shear which may lead to sea bed erosion. The vertical wavelength of the baroclinic M_2 waves observed off the Porcupine Bank is, however, about 1000 m (Thorpe 1987*b*) and is larger than the scale over which N^2 is found to vary; most of this low-frequency variability (on the Hebrides slope) is close to the sea bed. Although the variation of near-bed gradients may effect the boundary layer and the depth of mixing, it is unlikely to have much influence on wave reflection except for incident waves with vertical wavenumbers higher than those of the baroclinic tide, or very close to critical conditions, when the reflected wave will have very high wavenumber and hence propagate within the region in which the density gradient has been modified by the low-frequency slope waves.

We thank Dr John Gould for deploying and recovering the mooring on the Hebrides slope. The moorings off the Porcupine slope were laid in collaboration with the Institute of Oceanographic Sciences, Deacon Laboratory and we are most grateful for this cooperation

PHILOSOPHICAL TRANSACTIONS OF THE ROYAL SOCIETY A MATHEMATICAL, PHYSICAL & ENGINEERING SCIENCES

and, in particular, to the Masters and Crews of the NERC research vessels involved in the observational programme.

References

Armi, L. & D'Asaro, E. 1980 Flow structures of the benthic ocean. *J. geophys. Res.* **85**, 469–484.

Baines, P. G. 1973 The generation of internal tides by flat-bump topography. *Deep Sea Res.* **20**, 179–205.

Baines, P. G. 1974 The generation of internal tides over steep continental slopes. *Phil. Trans. R. Soc. Lond.* A **227**, 27–58.

Boyer, D. L. & Tao, L. 1987 On the motion of linearly stratified rotating fluids past capes. *J. Fluid Mech.* **180**, 429–449.

Cacchione, D. & Wunsch, C. 1974 Experimental study of internal waves over a slope. *J. Fluid Mech.* **66**, 223–240.

Dickson, R. R. & Kidd, R. B. 1986 Deep circulation in the southern Rockall Trough – the oceanographic setting of site 610. In *Initial reports of the deep-sea drilling project* XCIV, pp. 1061–1074. Washington, D.C.: U.S. Government Printing Office.

Ellett, D. J., Edwards A. & Bowers, R. 1986 The hydrography of the Rockall Channel – an overview. *Proc. R. Soc. Edinb.* B **88**, 61–81.

Eriksen, C. C. 1982 Observations of internal wave reflection off sloping bottoms. *J. geophys. Res.* **87**, 525–538.

Eriksen, C. C. 1985 Implications of ocean bottom reflection for internal wave spectra and mixing. *J. phys. Oceanogr.* **15**, 1145–1156.

Garrett, C. & Gilbert, D. 1988 Estimates of vertical mixing by internal waves reflected off a sloping bottom. In *Small-scale turbulence and mixing in the ocean* (ed. C. J. Nihoul & B. M. Jamart), pp. 405–424. Amsterdam: Elsevier.

Gilbert, D. & Garrett, C. 1989 Implications for ocean mixing of internal wave scattering off irregular topography. *J. Phys. Oceanogr.* **19**, 1716–1729.

Gill, A. E. 1982 *Atmosphere–ocean dynamics*. London: Academic Press. (622 pages.)

Huthnance, J. M. 1978 On coastally trapped waves; analysis and numerical calculation by inverse iteration. *J. phys. Oceanogr.* **8**, 74–92.

Huthnance, J. M. 1986 The Rockall slope current and shelf-edge processes. *Proc. R. Soc. Edinb.* B **88**, 83–801.

Huthnance, J. M., Mysak, L. A. & Wang, D.-P. 1986 Coastal trapped waves. Baroclinic processes on continental shelves. *Coastal Estuarine Sci.* **3**, 1–18.

Ivey, G. N. 1987 Boundary mixing in a rotating stratified fluid. *J. Fluid Mech.* **183**, 25–44.

Ivey, G. N. & Nokes, R. I. 1989 Vertical mixing due to the breaking of critical internal waves on sloping boundaries. *J. Fluid Mech.* **204**, 479–500.

Müller, P. 1988 Vortical motions. In *Small-scale turbulence and mixing in the ocean* (ed. J. C. J. Nihoul & B. M. Jamart), pp. 285–301. Amsterdam: Elsevier.

Norris, S. & MacDougall, N. 1986 Current meter observations near the Porcupine Bank, 1981–1983. *Fisheries Research Data rep.* no. 8, Lowestoft: MAFF.

Owens, W. B. & Hogg, N. G. 1980 Oceanic observations of stratified Taylor columns near a bump. *Deep Sea Res.* **27**, 1029–1045.

Phillips, O. M., Shyu, J.-H. & Salmun, H. 1986 An experiment on boundary mixing: mean circulation and transport rates. *J. Fluid Mech.* **173**, 473–499.

Pingree, R. D. & New, A. L. 1989 Downward propagation of internal tidal energy into the Bay of Biscay. *Deep Sea Res.* **36**, 735–758.

Prinsenberg, S. J. & Rattray, M. 1975 Effects of continental slope and variable Brunt-Vaisala frequency on the coastal generation of internal tides. *Deep Sea Res.* **22**, 251–263.

Thorpe, S. A. 1983 Benthic observations on the Madeira Abyssal Plain: fronts. *J. phys. Oceanogr.* **13**, 1430–1440.

Thorpe, S. A. 1987*a* On reflection of a train of finite-amplitude internal waves from a uniform slope. *J. Fluid Mech.* **178**, 279–302.

Thorpe, S. A. 1987*b* Current and temperature variability on the continental slope. *Phil. Trans. R. Soc. Lond.* A **323**, 471–517.

Thorpe. S. A. 1988 Benthic boundary layers on slopes. In *Small-scale turbulence and mixing in the ocean* (ed. J. C. J. Nihoul & B. M. Jamart), pp. 425–434. Amsterdam: Elsevier.

Thorpe, S. A. 1989 The distortion of short internal waves produced by a long wave, with application to ocean boundary mixing. *J. Fluid Mech.* **208**, 395–415.

Weatherly, G. L. & Martin, P. J. 1978 On the structure and dynamics of the oceanic bottom boundary layer. *J. phys. Oceanogr.* **8**, 557–570.

de Witt, L. N., Levine, M. D., Paulson, C. A. & Bert, W. V. 1986 Semi-diurnal internal tide in JASIN: observation and simulations. *J. geophys. Res.* **91**, 2581–2592.

Wunsch, C. & Hendry, R. 1972 Array measurements of the bottom boundary layer and the internal wave field on the continental slope. *Geophys. Fluid Dyn.* **4**, 101–145.

PHILOSOPHICAL TRANSACTIONS OF THE ROYAL SOCIETY A MATHEMATICAL, PHYSICAL & ENGINEERING SCIENCES